Advances in Military Technology
Vol. 17, No. 2, 2022, pp. 383-396
ISSN 1802-2308, eISSN 2533-4123
DOI 10.3849/aimt.01553

Novel Solution of Topological Recognition of Indoor Objects Based on Optical Flow and Planar Attributes

M. Ngoc Anh*

Le Quy Don Technical University, 236 Hoang Quoc Viet, Hanoi, Vietnam

The manuscript was received on 15 December 2021 and was accepted after revision for publication as research paper on 21 November 2022.

Abstract:

An approach of qualitative optical flow processing for indoor object recognition based on planar attributes is presented. The qualitative processing is performed under hierarchical segmentations of optical flow vectors. The proposed solution for indoor object recognition is undertaken from identifying planar and atilt properties of optical flow images. The advantages of the proposed solutions are the use of much simpler arithmetic to obtain more 3D details about indoor objects.

Keywords:

hierarchical segmentation, optical flow-based recognition, two-plane-built objects

1 Introduction

According to [1], the fourth revolution is a new era in which industry will deal with technologies like Robotics, Automation, Artificial Intelligence (AI), and others. Since 2011, the concept of industrial revolution 4.0 has gained popularity and inspired many scientific studies in robotics becoming smarter and closer to human thinking.

In robotics, mobile robot plays a very important role in many fields; not only industrial robots [2], but also agricultural [3], medical [4], and other service robots [5]. Mobile robots are required to move around the environment map, locate and plan the route between locations. Some of them have built-in cameras to handle mapping, planning, localizing and avoiding obstacle issues. There are many pairs of distinctly independent issues such as indoor [6] and outdoor [7] navigations, structured [8] and unstructured [9] environments, qualitative [10] and quantitative [11] image processing, metric [12] and topological [13] reconstruction. They may intertwine in specific research contexts.

* *Corresponding author: Advanced Technology Center, Le Quy Don TU, Hoang Quoc Viet str. 236, Bac Tu Liem district, Hanoi, Vietnam. Phone: (+84)-977-491277, E-mail: maingocanh@lqdtu.edu.vn. ORCID 0000-0002-0422-7195.*

Normally, for working in indoor environment, vision-based mobile robots have to cope with both structured and unstructured objects. Therefore, reconstructing typical geometrical models of the structured environments and dealing with obstacles in narrow spaces are the most important problems for indoor navigation. According to [12], vision-based depth reconstruction is a challenging problem extensively studied in computer vision but still lacking universal solution. Furthermore, reconstructing depth from single image is particularly valuable to mobile robotics as it can be embedded to the modern vision-based simultaneous localization and mapping methods providing them with the metric information needed to construct accurate maps in real scale. Especially, a number of optical flow-based solutions have been developed for vision-based robot navigation, e.g. [14] and [15]. These approaches, however, use complex computations based on quantitative (metric) decision making implementations.

To reduce complex computations, some other approaches propose qualitative solutions for optical flow processing to reconstruct situations, e.g. [16] and [17]. The limitations of these solutions are poor recognition of situations and infirm robustness to image noise of the working environment. Some others can find out obstacle details from the optical flow [15, 18] or indoor object recognition [19, 20]. These approaches, however, are not able to detect both indoor landmarks and obstacles simultaneously.

In this study, a solution of qualitative optical flow processing for indoor object recognition based on planar attributes is performed under hierarchical segmentations of optical flow vectors.

The proposed solutions are the use of much simpler arithmetic, the consumption of less computing time, and especially the recognition of more 3D details about indoor objects in the working environment.

The paper is organized as follows: Firstly, a vision-based mobile robot control system is briefly introduced; after that, the proposed solution of topological recognition of planar attribute-based structures is deeply focused on; finally, the experimental results of the qualitative optical flow processing are analyzed.

2 Vision-Based Mobile Robot Control System

2.1 Basic Concepts

This research focuses on four basic indoor landmarks including walls, corners, doors and corridors because they have relatively stable shapes in most buildings.

In 2D images, they are able to be illustrated by two planes as in the illustrations in Fig. 1 and they are named two-plane-built objects (TPO). The planar and atilt attributes of the TPOs will be computed for structurally recognizing 3D objects from 2D images.

The atilt attribute is presented via tilt angles. Tilt angle is defined as an angle φ between the line of sight (LOS) planes and flat object (FO) shown in Fig. 2. The plane LOS is a vertical plane ($\angle$ZOY) on the direct line between an observer (camera, robot) and a flat object. The plane FO is a vertical plane ($\angle$ZOX') containing the flat object, where axes X and Y are perpendicular, but X' and Y are not perpendicular.

2.2 Modular Diagram of Optical Flow-Based Mobile Robot System

To detect TPO, an optical flow-based object recognition in topological way is adopted rather than metric way in conventional solutions based on geometrical maps. The proposed topological solution for optical flow-based object recognition provides the results of optical flow-based recognition of distinctive objects that play the role of landmarks in navigation missions concerning path planning and obstructive objects. It is assumed that in the working environment, any object which is not used for path planning missions must be considered as an obstacle related to collision avoidance ones.

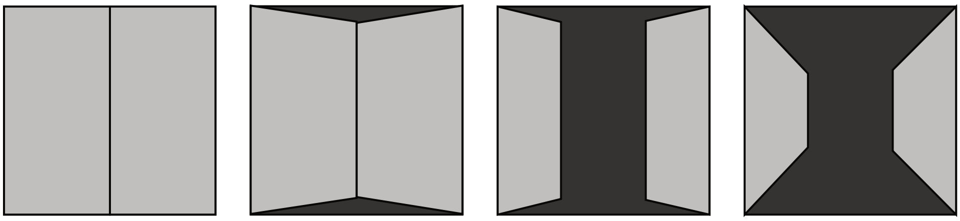

a) b) c) d)

Fig. 1 Arrangement of two planes to illustrate indoor objects: a) wall; b) corner; c) door; d) corridor

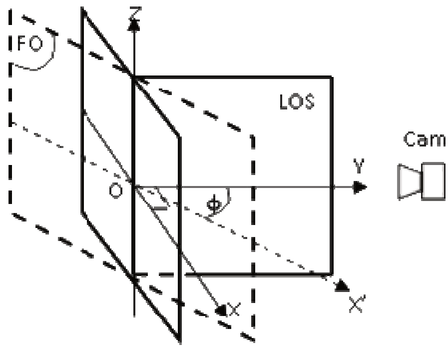

Fig. 2 Definition of tilt angle

The modular control system for vision-based mobile robot is implemented in a human way of thinking by using Fuzzy Inference Systems (FIS) at different levels of operation, as shown in Fig. 3. In the system, the optical flow processor performs functions of image processing to deliver optical flow vectors. Specifically, a 2D-correlation based block-matching approach for optical flow computation is used.

Module OFFIS executes object recognition based on the translational components of optical flow, which contains 3D information. This module computes also the distance to objects based on the relationship with optical flow magnitude and linear velocity of the mobile robot. Outputs of the object recognition and distance calculation are *obstacle distance*, *obstacle direction*, *TPO distance* and *TPO shape* supported for subsequent modules PAPFIS and MOFIS.

Module PAPFIS performs two missions of path planning including global and local path planning. In the global one, PAPFIS uses user-defined information including a topological map and mission objective to calculate a sequence of waypoints considered as a global path or trajectory. Otherwise, in the local one, PAPFIS identifies a local goal and navigates mobile robot to the local goal. The outputs of PAPFIS are *goal-oriented velocity* and *goal-oriented angle*.

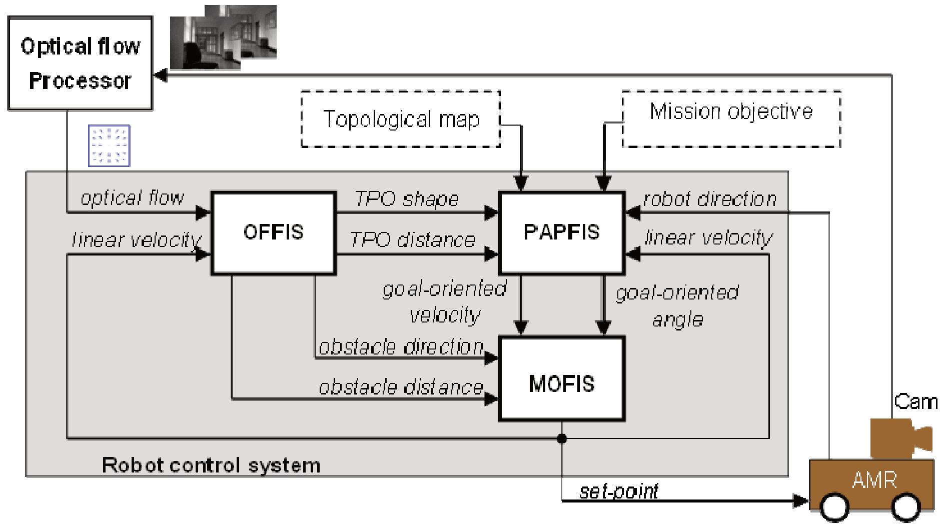

Fig. 3 Block diagram of optical flow-based mobile robot system

Module MOFIS computes a behavior to help the mobile robot avoid collision during travelling. Additionally, MOFIS executes a kinematic fusion between two behaviors of collision avoidance and goal orientation. The fuzzy-based fusion allows the mobile robot to smoothly travel in complex and changing environments. The output of MOFIS is a *set-point* command including *linear velocity* and *angular velocity* provided for the locomotion of the autonomous mobile robot (AMR).

2.3 Model Design of the Optical Flow-Based Object Recognition

In this research, the optical flow-based object recognition is executed in qualitative way in module OFFIS based on hierarchical segmentations of optical flow fields. The block diagram of OFFIS is designed as shown in Fig. 4 with six sub-modules including hierarchical segmentation, outlier removal filter, quadrant averaging, structural recognition, distance calculation, and situation determination.

Firstly, the optical flow is hierarchically segmented into rectangle quadrants. Secondly, the outlier removal filter eliminates optical flow outliers overwhelming dynamic thresholds that are automatically generated from averaging amplitudes of optical flow vectors in examined quadrants (we will present the new solution of outlier removal filter in a next paper). After removing outliers, the retained vectors are averaged and arranged in matrixes to identify planar and atilt properties that are necessary for reconstructing situation. Finally, a fuzzy-based situation determination is performed to create the shape of encountered TPO object and position of obstacle.

3 Solution of Planar Attribute-Based Structure Recognition

3.1 Hierarchical Segmentation

The whole field of optical flow is hierarchically segmented as the illustration in Fig. 5 with three layers of segmentation. In layer 1, optical flow is segmented into four quadrants Q_1, Q_2, Q_3 and Q_4, illustrated in Fig. 5a. In layer 2, all of the layer-1 quadrants are deeply segmented into layer-2 quadrants Q_{1i}, Q_{2i}, Q_{3i} and Q_{4i}, where i = 1…4, illustrated in Fig. 5b. In layer 3, all of the layer-2 quadrants are segmented into layer-3 quadrants Q_{1ij}, Q_{2ij}, Q_{3ij} and Q_{4ij}, where i = 1…4 and j = 1…4, shown in Fig. 5c. This progress is similar to an activity of zooming in.

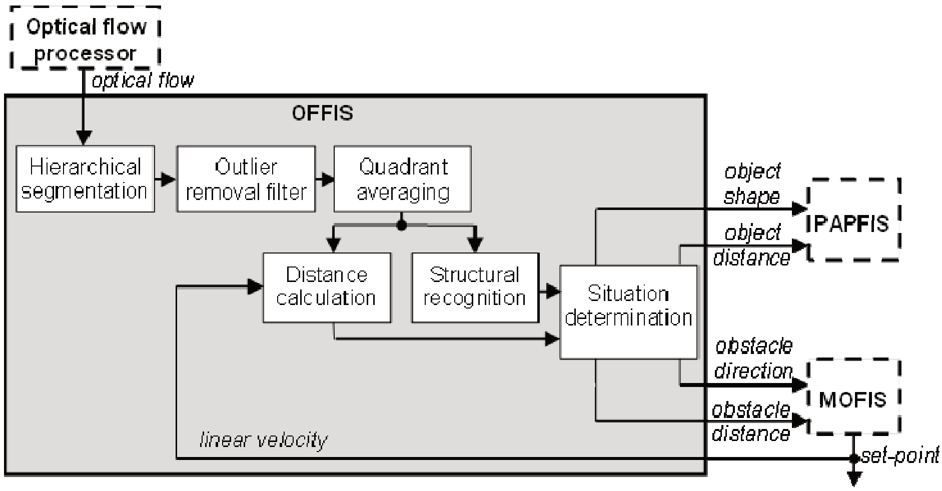

Fig. 4 Block diagram of module OFFIS

Mathematically, these quadrants can be arranged into the matrices as follows:

$$\left.\begin{aligned}
\boldsymbol{\Omega}^{\mathrm{I}} &= \begin{bmatrix} Q_1 & Q_2 \\ Q_3 & Q_4 \end{bmatrix} \\
\boldsymbol{\Omega}^{\mathrm{II}} &= \begin{bmatrix} Q_{11} & Q_{12} & Q_{21} & Q_{22} \\ Q_{13} & Q_{14} & Q_{23} & Q_{24} \\ Q_{31} & Q_{32} & Q_{41} & Q_{42} \\ Q_{33} & Q_{34} & Q_{43} & Q_{44} \end{bmatrix} \\
\boldsymbol{\Omega}^{\mathrm{III}} &= \begin{bmatrix} Q_{111} & Q_{112} & \cdots & Q_{221} & Q_{222} \\ Q_{113} & Q_{114} & \cdots & Q_{223} & Q_{224} \\ \vdots & \vdots & \ddots & \vdots & \vdots \\ Q_{331} & Q_{332} & \cdots & Q_{441} & Q_{442} \\ Q_{333} & Q_{334} & \cdots & Q_{443} & Q_{444} \end{bmatrix}
\end{aligned}\right\} \qquad (1)$$

where $\boldsymbol{\Omega}^{\mathrm{I}}$, $\boldsymbol{\Omega}^{\mathrm{II}}$, and $\boldsymbol{\Omega}^{\mathrm{III}}$ are matrices of average amplitude of optical flow vectors in layer-1 quadrants, layer-2 quadrants, and layer-3 quadrants, respectively.

Additionally, to detect position of obstacle, it is zoomed in only the quadrant(s) concerning the obstruction that owns the biggest average amplitude.

For example, in the situation shown in Fig. 6a, quadrant Q_3 covers the nearest obstacle. It means that the average amplitude of Q_3 is the biggest one. Therefore, a further segmentation is executed in quadrant Q_3 to obtain four layer-2 quadrants Q_{31}, Q_{32}, Q_{33} and Q_{34} like Fig. 6b. By relative comparing the average amplitudes of the layer-2 quadrants, it is determined that quadrant Q_{34} contains the nearest part of the obstacle. For this reason, quadrant Q_{34} will be intensely segmented into four smaller patterns called layer-3 quadrants Q_{341}, Q_{342}, Q_{343} and Q_{344} as in the illustration in

Fig. 6c. After segmenting into three layers, it is possible to exactly identify position of the obstacle in (8×8) matrix $\boldsymbol{\Omega}^{\mathrm{III}}$.

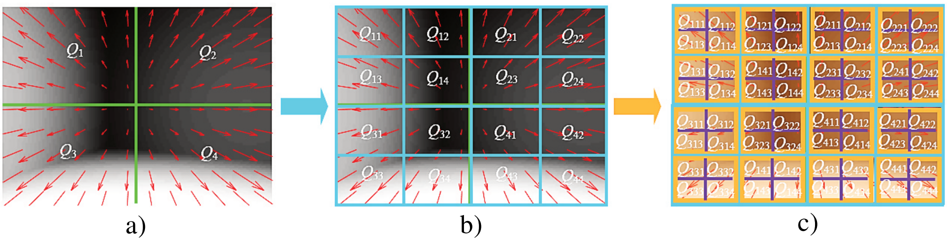

Fig. 5 Hierarchical segmentation in three layers
a) layer-1 segmentation, b) layer-2 segmentation, c) layer-3 segmentation

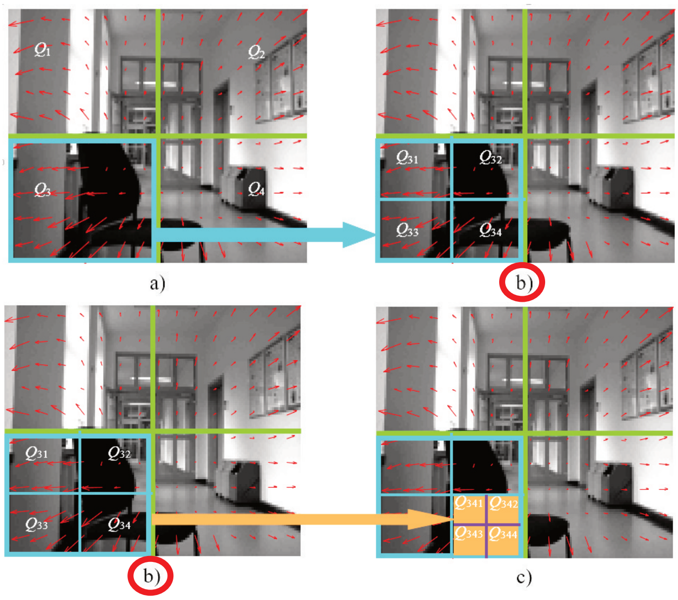

Fig. 6 Hierarchical segmentation for identifying obstacle position:
a) layer-1 quadrants, b) layer-2 quadrants, c) layer-3 quadrants

3.2 Planar Attribute Identification

Planar attributes are identified by comparing average amplitudes of two adjacent quadrants. There are two kinds of plane: vertical plane and horizontal plane. Vertical plane formed between two adjacent quadrants Q_{i} and Q_{j} in a column of the matrices $\boldsymbol{\Omega}$ in equation (1). Vertical plane is defined as

$$\mathrm{vplane}(Q_i, Q_j) = \begin{cases} 1 & \Leftrightarrow \mu_{\mathrm{U}i} \approx \mu_{\mathrm{U}j} \\ 0 & \Leftrightarrow \mu_{\mathrm{U}i} \neq \mu_{\mathrm{U}j} \end{cases} \tag{2}$$

where $\mu_{\mathrm{U}i}$ and $\mu_{\mathrm{U}j}$ are U-axis-projected average amplitudes of optical flow vectors in the two vertically adjacent quadrants.

Horizontal plane is formed between two adjacent quadrants Q_i and Q_j in a row of the $\boldsymbol{\Omega}$ in Eq. (1). Horizontal plane is defined as

$$\mathrm{hplane}(Q_i, Q_j) = \begin{cases} 1 & \Leftrightarrow \mu_{\mathrm{V}i} \approx \mu_{\mathrm{V}j} \\ 0 & \Leftrightarrow \mu_{\mathrm{V}i} \neq \mu_{\mathrm{V}j} \end{cases} \tag{3}$$

where $\mu_{\mathrm{V}i}$ and $\mu_{\mathrm{V}j}$ are V-axis-projected average amplitudes of optical flow vectors in the two horizontally adjacent quadrants.

If we compute all vertical and horizontal planes on matrices $\boldsymbol{\Omega}^{\mathrm{II}}$ and $\boldsymbol{\Omega}^{\mathrm{III}}$, we have respectively matrices ***vplaneL2***, ***hplaneL2***, ***vplaneL3***, and ***hplaneL3***:

$$\boldsymbol{vplaneL2} = \begin{bmatrix} \mathrm{vplane}(Q_{11}, Q_{13}) & \mathrm{vplane}(Q_{12}, Q_{14}) & \mathrm{vplane}(Q_{21}, Q_{23}) & \mathrm{vplane}(Q_{22}, Q_{24}) \\ \mathrm{vplane}(Q_{31}, Q_{33}) & \mathrm{vplane}(Q_{31}, Q_{34}) & \mathrm{vplane}(Q_{41}, Q_{43}) & \mathrm{vplane}(Q_{42}, Q_{44}) \end{bmatrix} \tag{4}$$

$$\boldsymbol{hplaneL2} = \begin{bmatrix} \mathrm{hplane}(Q_{11}, Q_{12}) & \mathrm{hplane}(Q_{21}, Q_{22}) \\ \mathrm{hplane}(Q_{13}, Q_{14}) & \mathrm{hplane}(Q_{23}, Q_{24}) \\ \mathrm{hplane}(Q_{31}, Q_{32}) & \mathrm{hplane}(Q_{41}, Q_{42}) \\ \mathrm{hplane}(Q_{33}, Q_{34}) & \mathrm{hplane}(Q_{43}, Q_{44}) \end{bmatrix} \tag{5}$$

$$\boldsymbol{vplaneL3} = \begin{bmatrix} \mathrm{vplane}(Q_{111}, Q_{113}) & \ldots & \mathrm{vplane}(Q_{222}, Q_{224}) \\ \mathrm{vplane}(Q_{131}, Q_{133}) & \ldots & \mathrm{vplane}(Q_{242}, Q_{244}) \\ \mathrm{vplane}(Q_{311}, Q_{313}) & \ldots & \mathrm{vplane}(Q_{422}, Q_{424}) \\ \mathrm{vplane}(Q_{331}, Q_{333}) & \ldots & \mathrm{vplane}(Q_{442}, Q_{444}) \end{bmatrix} \tag{6}$$

$$\boldsymbol{hplaneL3} = \begin{bmatrix} \mathrm{hplane}(Q_{111}, Q_{112}) & \cdots & \mathrm{hplane}(Q_{221}, Q_{222}) \\ \vdots & \ddots & \vdots \\ \mathrm{hplane}(Q_{333}, Q_{334}) & \cdots & \mathrm{hplane}(Q_{443}, Q_{444}) \end{bmatrix} \tag{7}$$

3.3 Atilt Attribute Identification

The tilt angle of a plane is calculated by the following equation

$$\mathrm{tilt}(Q_i, Q_j) = k_{\mathrm{Tilt}} \frac{\mu_{\mathrm{V}i}}{\mu_{\mathrm{V}j}} \tag{8}$$

where k_{Tilt} is a multiplier defined by the user to map tilt value to fuzzy range, e.g. [0, 1].

Using Eq. (8) to compute tilt angles on the two first and two last columns of the matrix $\boldsymbol{\Omega}^{\mathrm{II}}$ and $\boldsymbol{\Omega}^{\mathrm{III}}$, the matrix ***tiltL2*** and ***tiltL3*** are respectively defined as follows

$$\boldsymbol{tiltL2} = \begin{bmatrix} \mathrm{tilt}(Q_{11}, Q_{12}) & \mathrm{tilt}(Q_{22}, Q_{21}) \\ \mathrm{tilt}(Q_{13}, Q_{14}) & \mathrm{tilt}(Q_{24}, Q_{23}) \\ \mathrm{tilt}(Q_{31}, Q_{32}) & \mathrm{tilt}(Q_{42}, Q_{41}) \\ \mathrm{tilt}(Q_{33}, Q_{34}) & \mathrm{tilt}(Q_{44}, Q_{43}) \end{bmatrix} \tag{9}$$

$$\boldsymbol{tiltL3} = \begin{bmatrix} \mathrm{tilt}(Q_{111}, Q_{112}) & \mathrm{tilt}(Q_{222}, Q_{221}) \\ \mathrm{tilt}(Q_{113}, Q_{114}) & \mathrm{tilt}(Q_{224}, Q_{223}) \\ \vdots & \vdots \\ \mathrm{tilt}(Q_{331}, Q_{332}) & \mathrm{tilt}(Q_{442}, Q_{441}) \\ \mathrm{tilt}(Q_{333}, Q_{334}) & \mathrm{tilt}(Q_{444}, Q_{443}) \end{bmatrix} \tag{10}$$

DOI 10.3849/aimt.01553

4 Topological Recognition of Indoor Objects

4.1 Rough Topological Structures of Indoor Landmarks

Indoor landmarks are objects that have the ability to visually recognize the context of the surrounding context and determine its relative position in that context. In this research, four typical indoor landmarks are considered including doors, corners, corridors, and floors as mentioned in section 2.1.

The structural recognition is executed in a topological way by comparing the average amplitudes among the quadrants to identify the nearest quadrant, then using planar attributes to identify the nearest area, and finally masking the nearest area by 1 and the others by 0.

The rough structural recognition is performed on matrices $\boldsymbol{\Omega}^{\mathrm{II}}$, ***vplaneL2*** and ***hplaneL2***. Rough structural recognition is executed on layer 2 via three steps:

- comparing the layer-2 quadrants $Q_{ij}\big|_{j=1..4}$ of a layer-1 quadrant Q_i from each other to determine the closest quadrant with the biggest average $\mu_{ij\max}$,
- computing $\mathrm{vplane}\left(Q_{ij},Q_{i(j+2)}\right)$ and $\mathrm{hplane}\left(Q_{ij},Q_{i(j+1)}\right)$ to localize the closest area containing the closest quadrants,
- masking the closest area by 1 and the others by 0.

For example, the rough structural recognition of the situation illustrated in Fig. 7 is processed as the following:

- comparing $Q_{1j}\big|_{j=1..4}$ in Q_1 to figure out Q_{11} is the closest one,
- computing $\mathrm{vplane}\left(Q_{11},Q_{13}\right)=1$, so the closest area in Q_1 contains Q_{11} and Q_{13},
- masking the closest areas with 1, and others with 0.

The process is looped for Q_2, Q_3 and Q_4. Finally, the rough structure is formed as

$$\boldsymbol{roughS}_{\mathrm{Fig.7}}=\begin{bmatrix}1&0&0&1\\1&0&0&1\\1&0&0&1\\1&0&0&1\end{bmatrix} \tag{11}$$

4.2 Fine Topological Structures of Indoor Landmarks

The fine structural recognition is performed on matrices $\boldsymbol{\Omega}^{\mathrm{III}}$, ***vplaneL3*** and ***hplaneL3***. Similar to the rough structural recognition, the fine structural one is executed on layer 3 also through three steps:

- comparing the layer-3 quadrants Q_{ijk} of a layer-2 quadrant Q_{ij} from each other to determine the closest quadrant with the biggest average $\mu_{ijk\max}$,
- computing $\mathrm{vplane}\left(Q_{ijk},Q_{ij(k+2)}\right)$ and $\mathrm{hplane}\left(Q_{ijk},Q_{ij(k+1)}\right)$ to determine the closest area containing the closest quadrant,
- masking the closest area by 1 and the others by 0.

E.g., the matrix of fine structure recognition in the situation illustrated in Fig. 8 is

$$\boldsymbol{fineS}_{\text{Fig.8}} = \begin{bmatrix} 1 & 0 & \cdots & \cdots & 0 & 1 \\ 1 & 0 & \cdots & \cdots & 0 & 1 \\ \vdots & \vdots & \ddots & \ddots & \vdots & \vdots \\ \vdots & \vdots & \ddots & \ddots & \vdots & \vdots \\ 1 & 1 & \cdots & \cdots & 0 & 1 \\ 1 & 1 & \cdots & \cdots & 0 & 1 \end{bmatrix} \tag{12}$$

Finally, the matrices of rough and fine structure are supported for the subsequent module to determine shape of the encountered TPO and position of obstacle.

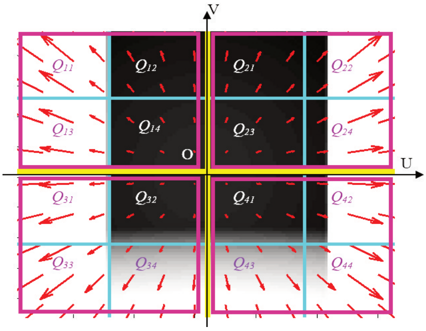

Fig. 7 Coping with a door

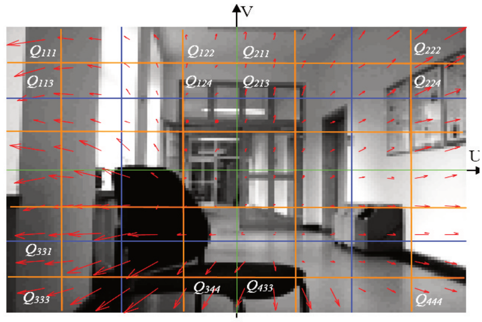

Fig. 8 Coping with a corridor and an obstacle

5 Experimental Results

Experiments have been performed in a real office environment under realistic conditions. The mobile robot used for all experiments is named IfAbot using a digital camera Logitech C310 HD with 1 280×720 screen resolution as the main sensor. Fig. 9 illustrates a scene of the experimental office environment.

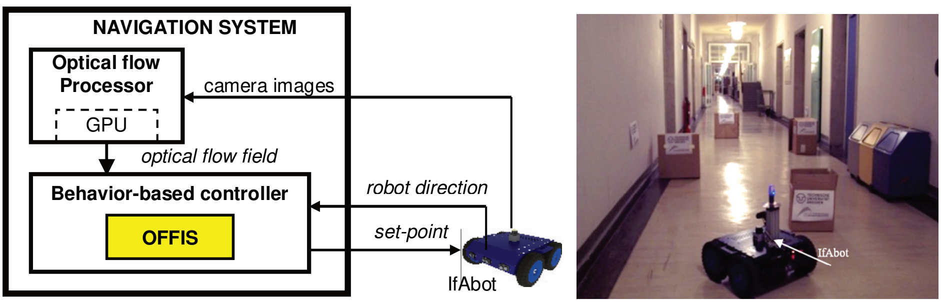

Fig. 9 Control system and scene of the experimental environment

Optical flow field for each image pair has been produced by a GPU NVIDIA GeForce GTX 260 1.24 GHz through a 2D correlation block matching algorithm with segment size 32×32 pixels. The size of optical flow vectors of each image is 16×16 (which is actually of low density) resulting in the following layer sizes: layer-1 quadrant contains 8×8, layer-2 quadrant contains 4×4 and layer-3 quadrant contains 2×2 flow vectors. The software for the experiments is written in Matlab source code and executed on a computer Intel(R) Pentium(R) 4 CPU 3.40 GHz.

DOI 10.3849/aimt.01553

In the experiments, the real office contains 3D indoor objects such as doors D*i*, rooms R*i*, and box-shaped obstacles along the corridor. The high level navigation task of IfAbot is to move from inside room R9 to the front of door D2 and avoiding all unknown artificial obstacles randomly arranged on the road. The colorful ground-truth and highlight images of the experiment are illustrated in Fig. 10. Especially, in Img4 the robot coped with 3 obstacles including 01 person and 02 boxes. The person is defined as the nearest obstacle due to its biggest average optical flow vector.

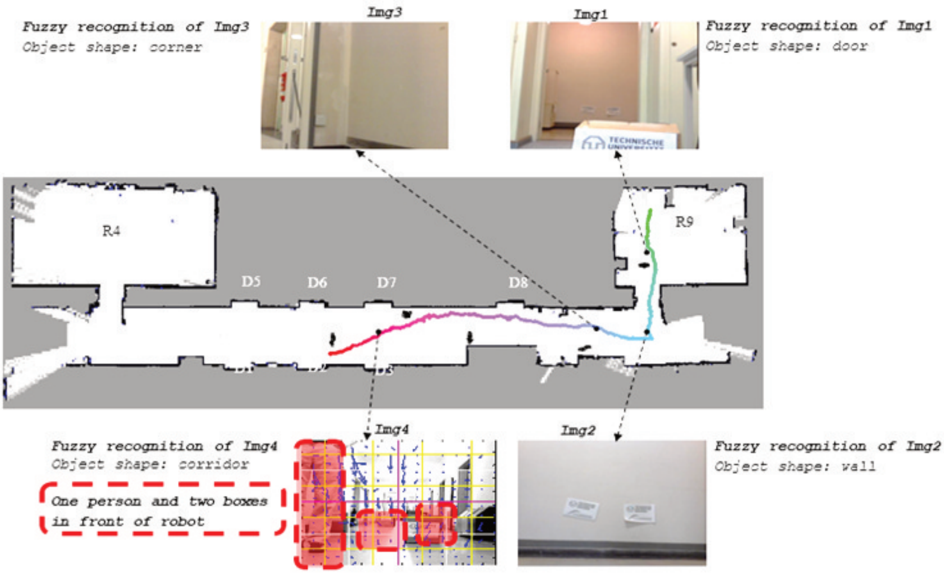

Fig. 10 Ground-truth and highlight images of moving from R9 to D2

The system for the recognizing of indoor object shapes based on Mamdani-type fuzzy membership functions is shown in Fig. 11. The system has 5 modules consisting of 01 rough classifier, 03 fine classifiers and 01 TPO decision module.

The fuzzy rules of the rough classifier for recognizing of indoor object groups is listed in Fig. 12. The fuzzy rules of the fine classifiers for the recognizing of indoor object shapes are illustrated in Fig. 13. The TPO decision module selects a maximum value from the outputs of the fine classifiers to make the final decision about the TPO object to be recognized.

Some indoor object interpretations of highlighted optical flow images taken and processed during the experiments are illustrated in Fig. 14.

The experiment results demonstrate the successful use and reliable operation of optical flow-based pattern recognition using fuzzy logic in a real environment.

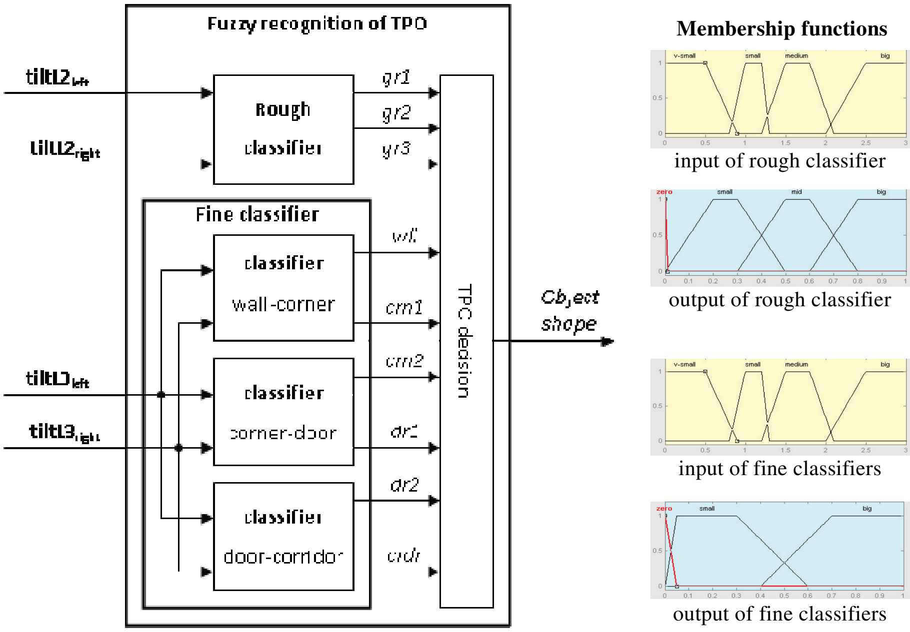

Fig. 11 Fuzzy-based recognition of indoor object shape

Fuzzy rules of rough classifier

IF	*THEN*
tL2_left v-small OR *tL2_right* v-small	*gr1* big AND *gr2* zero AND *gr3* zero
tL2_left small AND *tL2_right* small	*gr1* big AND *gr2* small AND *gr3* zero
tL2_left small AND *tL2_right* medium	*gr1* small AND *gr2* big AND *gr3* zero
tL2_left small AND *tL2_right* big	*gr1* zero AND *gr2* big AND *gr3* small
tL2_left medium AND *tL2_right* small	*gr1* small AND *gr2* big AND *gr3* zero
tL2_left medium AND *tL2_right* medium	*gr1* zero AND *gr2* big AND *gr3* mid
tL2_left medium AND *tL2_right* big	*gr1* zero AND *gr2* small AND *gr3* big
tL2_left big AND *tL2_right* small	*gr1* zero AND *gr2* big AND *gr3* small
tL2_left big AND *tL2_right* medium	*gr1* zero AND *gr2* small AND *gr3* big
tL2_left big AND *tL2_right* big	*gr1* zero AND *gr2* zero AND *gr3* big

Fig. 12 Fuzzy rules of rough classifier for recognizing of indoor object groups

Fig. 13 Fuzzy rules of fine classifier for recognizing of indoor object shapes

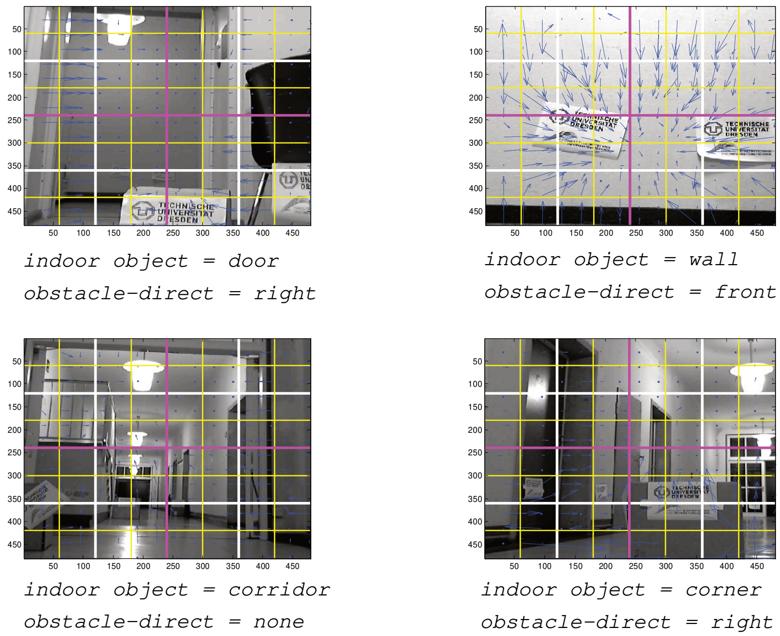

Fig. 14 Indoor object interpretations of highlighted optical flow images

6 Conclusions

This paper has presented the novel solution for indoor object recognition undertaken from identifying planar and atilt properties of optical flow images.

Compared with classical approaches of optical flow-based indoor object detection, this approach has some advantages of simultaneous recognition of multiple objects in the same optical flow image including indoor landmark and obstacles. In particular, the proposed solution of topological recognition uses much simpler arithmetic to obtain 3D details of the indoor objects.

Acknowledgement

The author thanks the German Academic Exchange Service DAAD and the Faculty of Automation of TU Dresden, Germany for financial support of the research.

References

[1] RUCHI G. and G. POOJA. Robotics and Industry 4.0. In: A. NAYYAR and A. KUMAR. *A Roadmap to Industry 4.0: Smart Production, Sharp Business and Sustainable Development*. Berlin: Springer, 2020, pp 157-169. ISBN 978-3-030-14543-9.

[2] GUO, S., Q. DIAO and F. XI. Vision Based Navigation for Omni-directional Mobile Industrial Robot. *Procedia Computer Science*, 2017, **105**, pp. 20-26. DOI 10.1016/j.procs.2017.01.182.

[3] AHMADI, A., L. NARDI, N. CHEBROLU and C. STACHNISS. Visual Servoing-based Navigation for Monitoring Row-Crop Fields. In: *IEEE International Conference on Robotics and Automation (ICRA).* New York: Cornell University, 2020.

[4] ÖZKIL, A.G. *Service Robots for Hospitals: Key Technical Issues* [PhD thesis]. Kongens Lyngby: Technical University of Denmark, 2011.

[5] GORDON, S.W., S. PANG, R. NISHIOKA, N. KASABOV and T. YAMAKAWA. Vision Based Mobile Robot for Indoor Environmental Security. In: KÖPPEN, M., N. KASABOV and G. COGHILL, eds. *Advances in Neuro-Information Processing*, *ICONIP*. Heidelberg: Springer, 2009, pp. 962-969. DOI 10.1007/978-3-642-02490-0_117.

[6] SHWE, L.L.T. and W.Y. WIN. Vision-Based Mobile Robot Self-localization and Mapping System for Indoor Environment. *American Scientific Research Journal for Engineering, Technology, and Sciences*, 2017, **38**(1), pp. 306-324. ISSN 2313-4410.

[7] JING P., W. ZHENG and Q. XU. Vision-based Mobile Robot's Environment Outdoor Perception. In: *Proceedings of the 3rd International Conference on Computer Science and Application Engineering*. New York: Association for Computing Machinery, 2019, pp. 1-5. DOI 10.1145/3331453.3361655.

[8] AL-MUTIB, K.N., A.M. EBRAHIM, M.M. ALSULAIMAN and H. RAMDANE. Stereo Vision SLAM based Indoor Autonomous Mobile Robot Navigation. In: *IEEE International Conference on Robotics and Biomimetics*. Bali: IEEE, 2014, pp. 1584-1589. DOI 10.1109/ROBIO.2014.7090560.

[9] LI, Y. Multimodal Visual Image Processing of Mobile Robot in Unstructured Environment Based on Semi-Supervised Multimodal Deep Network. *Journal of Ambient Intelligence and Humanized Computing*, 2020, **11**, pp. 6349-6359. DOI 10.1007/s12652-020-02037-4.

[10] KASSIR, M.M., M. PALHANG and M.R. AHMADZADEH. Qualitative Vision-Based Navigation Based on Sloped Funnel Lane Concept. *Intelligent Service Robotics*, 2020, **13**, pp. 235-250. DOI 10.1007/s11370-019-00308-4.

[11] PATRUNO, C., R. COLELLA, M. NITTI, V. RENÒ, N. MOSCA and E. STELLA. A Vision-Based Odometer for Localization of Omnidirectional Indoor Robots. *Sensors,* 2020, **20**(3), pp. 1-25. DOI 10.3390/s20030875.

[12] BOKOVOY A., K. MURAVYEV and K. YAKOVLEV. Real-time Vision-based Depth Reconstruction with NVidia Jetson. In: *European Conference on Mobile Robots (ECMR).* New York: Cornell University, 2019. DOI 10.48550/arXiv.1907.07210.

[13] BARBER R., J. CRESPO, C. GOMEZ, A.C. HERNÁNDEZ and M. GALLI. Mobile Robot Navigation in Indoor Environments: Geometric, Topological, and Semantic Navigation. In: E.G. HURTADO, ed. *Applications of Mobile Robots*. London: IntechOpen, 2019. ISBN 978-1-78985-755-4.

[14] SHAH, H.N.M.S, Z. KAMIS, M.F. ABDOLLAH, A. KHAMIS, M.S.M. ARAS, M.R. BAHARON and I.N. AZNI. Vision Based Obstacle Avoidance for Mobile Robot using Optical Flow Process. *International Journal of Innovative Technology and Exploring Engineering (IJITEE)*, **8**(4S), 2019, pp. 466-470. ISSN 2278-3075.

[15] NADOUR M., M. BOUMEHRAZ and L. CHERROUN. Mobile Robot Visual Navigation Based on Fuzzy Logic and Optical Flow Approaches. *International Journal of System Assurance Engineering and Management*, 2019, **10**, pp. 1654-1667. DOI 10.1007/s13198-019-00918-2.

[16] WANG, Y., P. WANG, Z. YANG, C. LUO, Y. YANG and W. XU. UnOS: Unified Unsupervised Optical-flow and Stereo-depth Estimation by Watching Videos. In: *IEEE/CVF Conference on Computer Vision and Pattern Recognition (CVPR).* Long Beach: IEEE, 2019, pp. 8071-8081. DOI 10.1109/CVPR.2019.00826.

[17] ALQUISIRIS-QUECHAAND, O. and J. MARTINEZ-CARRANZA. Depth Estimation Using Optical Flow and CNN for the NAO Robot. *Research in Computing Science*, 2019, **148**(11), pp. 49-58. DOI 10.13053/rcs-148-11-4.

[18] LIU, M. and T. DELBRUCK. ABMOF: A Novel Optical Flow Algorithm for Dynamic Vision Sensors [online]. 2018 [viewed 2021-10-02]. Available from: https://arxiv.org/pdf/1805.03988.pdf

[19] LÓPEZ-RUBIO, F.J. and E. LÓPEZ-RUBIO. Foreground Detection for Moving Cameras with Stochastic Approximation. *Pattern Recognition Letters*, 2015, **68**(P1), pp.161-168. DOI 10.1016/j.patrec.2015.09.007.

[20] SEKKAL, R., F. PASTEAU, M. BABEL, B. BRUN and I. LEPLUMEY. Simple Monocular Door Detection and Tracking. In: *IEEE International Conference on Image Processing*. Melbourne: IEEE, 2013, pp. 3929-3933. DOI 10.1109/ICIP.2013.6738809